Planetary waves: a numerical study of Rossby waves

Anna Lina P. Sjur and Jan-Adrian H. Kallmyr

December 14, 2018

Abstract

In this article, we study Rossby waves using different both implicit and explicit schemes for solving the wave equation numerically. We consider both the advantages and disadvantages of the methods, as well as their efficiency and accuracy. From this analysis, we find that the implicit scheme (centered) is more accurate and stable.

1 Introduction

We encounter wave phenomena everywhere in the natural sciences. From quantum mechanics to oceanography, we find that be it the motion of a particle or the ocean, we require knowledge of wave-like behaviour to solve the problem. In quantum mechanics, a particle's wave function is described by a complex-valued diffusion equation, the Schrödinger equation, while in oceanography, we can describe ocean waves using the wave equation,

$$\frac{\partial^2 u}{\partial x^2} = \frac{\partial^2 u}{\partial t^2}, \tag{1}$$

where x and t denote the spatial and temporal coordinates, respectively. The wave equation will be the topic of this paper, in particular, we will model Rossby waves, first identified by Rossby (1939). These are inertial, planetary waves in the Earth's atmosphere and ocean which motions contribute to extreme weather (Mann et al., 2017), might drive the El-Ninõ southern oscillation (ENSO) (Bosc and Delcroix, 2008), and is also produced by ENSO, see Battisti (1989). While we hope the reader appreciate the wide range of phenomena related to these waves, our article presents a numerical study of the waves isolated from other processes. We therefore begin by describing fundamental theory of waves and partial differential equations in the Theory section, present our algorithm and the technicalities relating to its implementation. In the Results section, we present our data as figures, before discussing their implications in the Discussion section. Concluding our paper, we present our final thoughts on the topic of simulating Rossby waves.

2 Theory

2.1 Wave analysis

Waves are solutions of the wave equation (see eq. 1), and have certain properties such as the phase velocity

$$v_p = \frac{\lambda}{T} = \frac{\omega}{k}, \tag{2}$$

where λ is the wavelength, T the period, ω the angular frequency and k the wavenumber. We found the phase velocity of a variety of waves graphically by studying Hovmöller diagrams (Hovmöller, 1949).

2.2 Rossby wave equation

Rossby waves are low frequency waves induced by the meridional variation of the Coriolis parameter f. This parameter depends on the rotation of the Earth Ω and the latitude φ, and is given by

$$f = \Omega \sin \varphi. \tag{3}$$

An approximation where f is set to vary linear in space is called the β-plane approximation, and can be written as

$$f = f_0 + \beta y, \tag{4}$$

where $\beta = \frac{df}{dy}\Big|_{\varphi_0} = \frac{2\Omega}{a}\cos\varphi_0$, a being the radius of the Earth. Combining the β-plane approximation with the shallow water vorticity equation, you get the quasi-geostrophic vorticity equation. This can be linearised, and by assuming a constant mean flow without bottom topography, you get the barotropic Rossby wave equation:

$$(\partial_t + U\partial_x)\nabla_H\psi + \beta\partial_x\psi = 0. \tag{5}$$

Here, ψ is the stream function describing the velocity perturbation, ∂_x denotes $\frac{\partial}{\partial x}$, ∇_H is the horizontal divergence $\partial x + \partial y$ and U is the mean velocity. In this report, we will assume no mean velocity, i.e. $U = 0$, in which case equation (5) simplifies to

$$\partial_t\nabla_H\psi + \beta\partial_x\psi = 0. \tag{6}$$

Two forms of boundaries will be examined in this report, that is periodic and constant boundaries. The first case can be used to describe an atmosphere that wraps around the earth, where the stream function is equal at the end-points. The latter case, where the stream function has a constant value at the boundaries, can be used to describe an ocean basin.

A possible solution to (6) in one dimension with periodic boundaries, where $x \in [0, L]$, is given by

$$\psi = A\cos(kx - \omega t), \tag{7}$$

where $k = \frac{2n\pi}{L}$ and $\omega = -\frac{\beta L}{2n\pi}$. The phase speed c can be calculated through the dispersion relation, given by

$$c = \frac{\omega L}{2n\pi} = -\beta\left(\frac{L}{2n\pi}\right)^2. \tag{8}$$

Since β is positive for all latitudes, the phase speed will be negative, implying that Rossby waves travels from east to west in a bounded domain.

The same problem, but with constant boundaries equal to zero, has the possible solution

$$\psi = A\sin\left(\frac{\pi n}{L}x\right)\cos(kx - \omega t), \tag{9}$$

with $k = \frac{L}{\pi n}$ and $\omega = -\frac{\beta}{2k}$. Here, the phase speed is given by

$$c = \frac{\omega L}{2n\pi} = -\frac{\beta}{4} \tag{10}$$

Again, the phase speed is negative. Equation (9) describes a cosine wave where the amplitude is dependent on the position, following a sine curve with zeros at the boundaries.

2.2.1 Differential equations

The forward difference is of first order, meaning that the error is proportional to Δt. The centred difference, on the other hand, is of second order, with an error proportional to Δt^2 for the time derivative and Δx^2 for the spatial derivative.

2.3 Discretisation and algorithm

Scaling eq. 6, we essentially wanted to solve two equations

$$\partial_t\zeta + \partial_x\psi = 0 \tag{11}$$

$$\partial_{xx}\psi = \zeta, \tag{12}$$

where the latter is Poisson's equation. To discretise, we use the following schemes:

$$\partial_q f \approx \frac{f_{q+1} - f_q}{\Delta q}, \tag{13}$$

$$\partial_q f \approx \frac{f_{q+1} - f_{q-1}}{2\Delta q}, \tag{14}$$

$$\partial_{qq} f \approx \frac{f_{q+1} - 2f_q + f_{q-1}}{(\Delta q)^2}, \tag{15}$$

where f is arbitrary and q a general coordinate. Here eq. 13 is the explicit forward scheme, and eq. 14 the implicit centered scheme. Letting $t^n = n\Delta t$ and $x_j = j\Delta x$, eq. 11 becomes

$$\zeta_j^{n+1} = \zeta_j^n - \frac{\Delta t}{2\Delta x}\left(\psi_{j+1}^n - \psi_{j-1}^n\right) \tag{16}$$

in the explicit scheme, and

$$\zeta_j^{n+1} = \zeta_j^{n-1} - \frac{\Delta t}{\Delta x}\left(\psi_{j+1}^n - \psi_{j-1}^n\right) \tag{17}$$

in the implicit scheme. For Poisson's equation, we simply have

$$\frac{\psi_{j+1}^{n+1} - 2\psi_j^{n+1} + \psi_{j-1}^{n+1}}{(\Delta x)^2} = \zeta_j^{n+1}. \tag{18}$$

Our general algorithm is then Algorithm **??**. What remains now is to determine how to solve

initialise ψ^0, ζ^0;
for $n = 0, 1, \ldots, \ T$ **do**
    for $j = 0, 1, \ldots, X$ **do**
        solve for ζ_j^{n+1};
        solve for ψ_j^{n+1};

Algorithm 1: Algorithm for solving the 1+1 dimensional Rossby wave equation. Here T and X are the grid sizes in the temporal and spatial dimensions respectively.

the equations for closed and periodic boundary conditions. In the case of closed boundaries we had the Dirichlet boundary conditions, and could use gaussian elimination as outlined in one of our earlier papers (Sjur and Kallmyr, 2018). As for the periodic domain, we found that the resulting matrix form of the Laplacian would be singular. This prompted us to implement Jacobi's method, as described by Hjorth-Jensen (2015).

Up until this point we had only considered the $1+1$ dimensional Rossby wave, however, expanding to $2+1$ dimensions was rather straightforward as we could employ the same Jacobi's method as for the one-dimensional case. Therefore, we won't go into anymore detail.

2.4 Implementation

We implemented our algorithms in C++ using the armadillo and LAPACK libraries to handle matrix operations. To analyse data and produce figures, we used python 3.6 with a standard set of modules: matplotlib, numpy and seaborn.

3 Results

Looking at Figure 1, we observe the time evolution of a sine wave in the periodic domain. We see that the wave is easterly (travelling towards the west). There are four distinct antinodes throughout the entire duration of the wave, and a wavelength is determined to be 0.5. After a time $t = 140$ we can see that the wave is in anti-phase to its initial state.

Considering now the bounded sine wave (Figure 2), the direction of propagation is still west, and the four anti-nodes look to be reduced by two, yielding only two anti-nodes at any point in time. We can approximate a wavelength to be 0.6. The same behaviour after time $t = 140$ is also observed here.

From Figure **??** we see that the periodic gaussian wave exhibits different behaviour

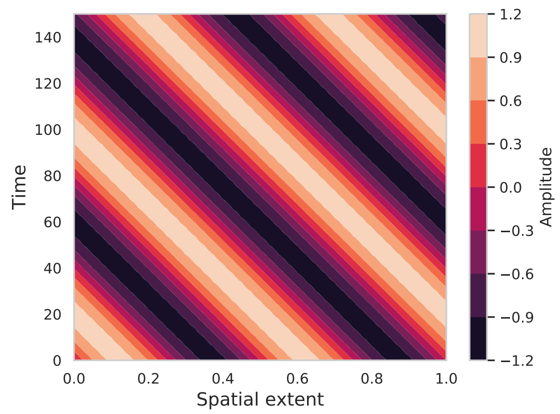

Figure 1: Hovmöller diagram of a Rossby wave with periodic boundary conditions, initially a sine wave using a implicit scheme, where $\Delta x = 0.025$ *and* $\Delta t = 0.1$.

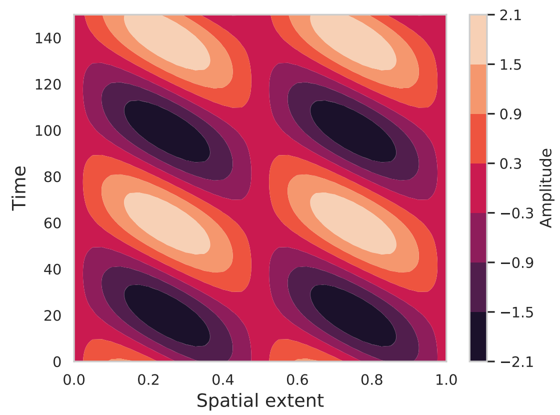

Figure 2: Hovmöller diagram of a bounded Rossby wave with a initial sine wave using a implicit scheme. Here $\Delta x = 0.025$ *and* $\Delta t = 0.1$.

caompared to the sine wave. There are at most two distinct anti-nodes at any point in time, and there looks to be a changing pattern in time, compared to the sine waves which always look the same. No wavelength can be discerned from the diagram.

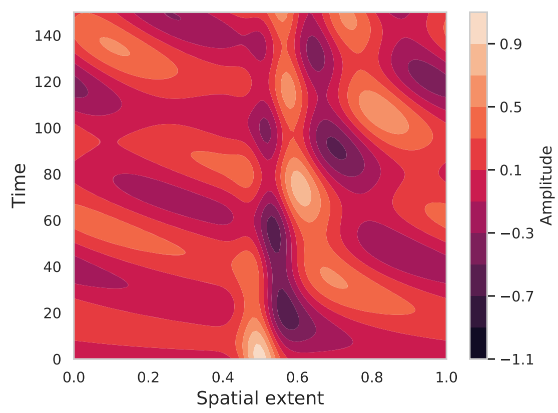

Figure 3: Hovmöller diagram of a Rossby wave with periodic boundary conditions, initially a centered gaussian ($x_0 = 0.5$) *using a implicit scheme. Here* $\sigma = 0.05$, $\Delta x = 0.01$ *and* $\Delta t = 0.1$.

In Figure 6 we show the Hovmöller diagram of a gaussian with closed boundaries. In this case, while there are still variations in time, we can clearly discern oscillations between minima and maxima.

4 Discussion

Looking back at the Hovmöller diagrams, we find that Figure 1 corresponds well with the analytical expression in eq. 7 as shown in the figure is the very distinct Hovmöller diagram for a cosine wave with a constant amplitude of 1. In the bounded case (Figure 2) we find that the amplitude oscillates with $\sin x$ as expected. Both waves are easterlies, which is as expected from the analytical negative dispersion relation

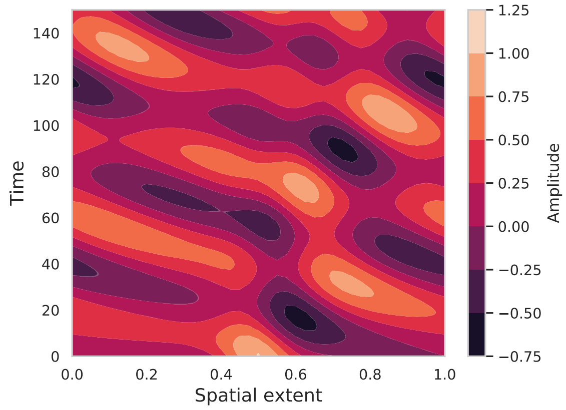

Figure 4: Hovmöller diagram of a Rossby wave with periodic boundary conditions, initially a centered gaussian ($x_0 = 0.5$) using a implicit scheme. Here $\sigma = 0.1$, $\Delta x = 0.025$ and $\Delta t = 0.1$.

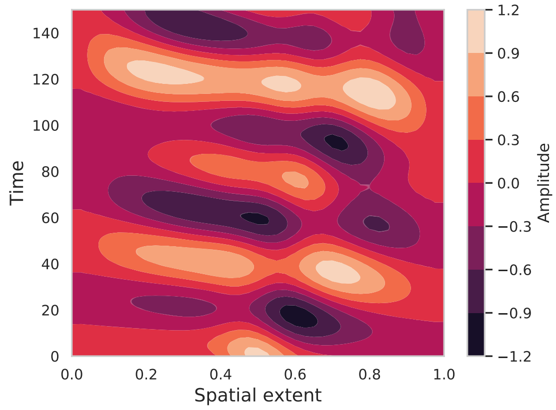

Figure 6: Hovmöller diagram of a bounded Rossby wave initially a centered gaussian ($x_0 = 0.5$) using a implicit scheme. Here $\sigma = 0.1$.

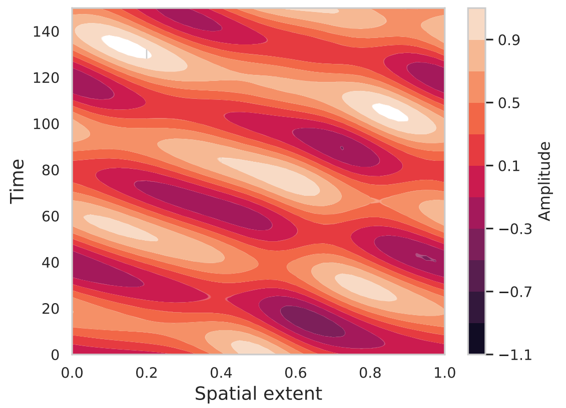

Figure 5: Hovmöller diagram of a Rossby wave with periodic boundary conditions, initially a centered gaussian ($x_0 = 0.5$) using a implicit scheme. Here $\sigma = 0.15$, $\Delta x = 0.025$ and $\Delta t = 0.1$.

$\mathbf{n}$	$\mathbf{t_g/t_s}$	$\mathbf{t_{LU}/t_s}$
10	2.08	3.70
10^2	1.89	$1.00 \cdot 10^2$
10^3	1.48	$1.05 \cdot 10^4$
10^4	1.43	$1.18 \cdot 10^6$
10^5	1.39	-
10^6	1.41	-
10^7	1.39	-

Table 1: Ratio between CPU time for the general algorithm ($\mathbf{t_g}$), the special algorithm ($\mathbf{t_g}$) and the LU decomposition algorithm ($\mathbf{t_{LU}}$) for different matrix sizes ($\mathbf{n}$). The LU decomposition crashed for $\mathbf{n}$ greater than 10^4.

(eq. 10), and correlates with Rossby's original observations (Rossby, 1939).

As for the gaussian waves, we have no analytical solutions, but find that

5 Conclusion

References

David S Battisti. On the role of off-equatorial oceanic rossby waves during enso. *Journal of physical Oceanography*, 19(4):551–560, 1989.

Christelle Bosc and Thierry Delcroix. Observed equatorial rossby waves and enso-related warm water volume changes in the equatorial pacific ocean. *Journal of Geophysical Research: Oceans*, 113(C6), 2008.

Morten Hjorth-Jensen. Computational physics. https://github.com/CompPhysics/ComputationalPhysics/blob/master/doc/Lectures/lectures2015.pdf, 2015.

Ernest Hovmöller. The trough-and-ridge diagram. *Tellus*, 1(2):62–66, 1949.

Michael E Mann, Stefan Rahmstorf, Kai Kornhuber, Byron A Steinman, Sonya K Miller, and Dim Coumou. Influence of anthropogenic climate change on planetary wave resonance and extreme weather events. *Scientific Reports*, 7:45242, 2017.

Carl-Gustaf Rossby. Relation between variations in the intensity of the zonal circulation of the atmosphere and the displacements of the semi-permanent centers of action. *J. Mar. Res.*, 2:38–55, 1939.

Anna Lina P. Sjur and Jan-Adrian H. Kallmyr. Two methods of solving linear second-order differential equations. https://github.com/janadr/FYS3150/blob/master/prosjekt1/tex/main.pdf, 2018.

A

$$A = \begin{bmatrix} b_1 & c_1 & 0 & \dots & \dots & 0 \\ a_1 & b_2 & c_2 & 0 & \dots & 0 \\ 0 & a_2 & b_3 & c_3 & \dots & 0 \\ \vdots & \ddots & \ddots & \ddots & \ddots & \vdots \\ 0 & \dots & \ddots & a_{n-2} & b_{n-1} & c_{n-1} \\ 0 & \dots & \dots & 0 & a_{n-1} & b_n \end{bmatrix},$$